Fuel 373 (2024) 132084

Contents lists available at ScienceDirect

Fuel

journal homepage: www.elsevier.com/locate/fuel

Full Length Article

Chemical composition and molecular structure of asphaltene in Azerbaijani crude oil: A case study of the Zagli field

Ulviyya Jeyhun Yolchuyeva [a,b,*], Vagif M. Abbasov [a], Rana Jafarova [a], Ayaz Mammadov [a,b], Saida Ahmadbayova [a], Ravan A. Rahimov [a,b,c], Alakbar Huseynzada [d,e,f], Fargana Alizadeh [a,e]

[a] Institute of Petrochemical Processes named after academician Y.H.Mammadaliyev of Ministry of Science and Education Republic of Azerbaijan, Khojali ave. 30, AZ1025, Baku, Azerbaijan
[b] Department of Chemical Engineering, School of Engineering and Applied Science, Khazar University, 41 Mahsati Str., AZ1096 Baku, Azerbaijan
[c] Department of Chemical Engineering, Baku Engineering University, Hasan Aliyev str. 120, Baku, Absheron AZ0101, Azerbaijan
[d] ICRL, Baku State University, Z. Khalilov 23, Baku, AZ 1148, Azerbaijan
[e] GPOGC SRI, Azerbaijan State Oil and Industry University, Baku, Azerbaijan
[f] ICESCO Biomedical Materials Chair, Baku State University, Z. Khalilov 23, Baku, AZ 1148, Azerbaijan

ARTICLE INFO

Keywords:
Zagli crude oil
Asphaltene
Molecular structure
Crystallite parameters
NMR
XRD

ABSTRACT

The lack of information about the chemical composition and structure of asphaltenes in crude oil, which has a sufficient share in the economy of Azerbaijan, complicates its processing and use. As a first attempt, this research is devoted to the detailed analysis of the average molecular structure and properties of asphaltenes isolated from crude oil samples collected from the Zaglı oil field using the integrated application of high-sensitivity devices such as Nuclear Magnetic Resonance (NMR), Ultraviolet–Visible (UV–Vis), Fourier Transform Infrared (FTIR) spectroscopy, X-ray diffraction analysis, Elemental analysis, Scanning Electron Microscope (SEM), Differential Thermal Analysis (DTA), Dynamic Light Scattering (DLS). The average molecular formula of asphaltene monomer was determined to be $C_{49.5}H_{55}O_{3.04}N_{0.95}S_2$. An island architecture with one polycyclic aromatic hydrocarbon (PAH) in each molecule of this compound is predominant. Amorphous asphaltene molecule contains vanadium-based porphyrins, –COOH group, disulfide (−S-S-) linkage. It was found that asphaltene of crude oil is stable up to 406 °C. The three-stage pyrolysis process in the temperature range of 406–818 °C resulted in the formation of 12.58 % coke. Due to the absence of free radicals in the range of 25–100 ℃, the asphaltene sample is dielectric. The decrease of monodispersity with particle growth in asphaltene compound in different solvents was analyzed by dynamic and static light scattering. The HOMO-LUMO energy gap of the asphaltene molecule was 2.666 eV, indicating high stability. The knowledge gained about the chemical composition and molecular structure of asphaltenes can help prevent problems arising in oil production and refining processes.

1. Introduction

The Republic of Azerbaijan is famous for its oil wells, which have a rich chemical composition. Since the 80 s of the last century, the study of the properties of oil and oil products (for example, composition, structure, spectral-luminescence, heat, etc.) made it possible to develop new technological schemes for purchasing affordable products (fuel, lubricants, etc.). On the other hand, it is known that the reprocessing of tar-asphalten substances contained in oil and oil residues is the basis of their efficient use.

The chemical composition and molecular structure of asphaltenes provide information on aggregation/precipitation processes. These processes cause serious problems in the oil industry and complicate the production and processing of oils [1–3]. Dickakian and Seay [4] showed that the main factors hindering the processes of thermal conversion of oil in an oil refinery are precipitation and carbonization of asphaltene. Undesirable carbonization negatively affects productivity and reduces economic efficiency in conversion processes by lowering heat transfer coefficients. Asphaltenes prevent the separation of water from oils, creating water–oil emulsions [5–7].

Asphaltenes are composed of condensed polycyclic aromatic hydrocarbons, molecules with heteroatoms, paraffin and naphthenic

* Corresponding author at: Institute of Petrochemical Processes of Ministry of Science and Education Republic of Azerbaijan, Khojali ave. 30, AZ1025, Baku, Azerbaijan.
E-mail address: u.jeyhunzade@gmail.com (U.J. Yolchuyeva).

https://doi.org/10.1016/j.fuel.2024.132084
Received 10 March 2024; Received in revised form 30 April 2024; Accepted 31 May 2024
Available online 22 June 2024

chains of various sizes, shapes and structures. These large molecules include carbon, hydrogen, nitrogen, oxygen, and sulfur, and small amounts of iron, vanadium, and nickel [8–12]. The amount of hydrogen and carbon in asphaltenes separated from various oils is in the range of 8.1 ± 0.7 % and 82 ± 3 %, respectively and the hydrogen/carbon (H/C) ratio, which is almost constant, is in the range of 1.15 ± 0.05 %. The amount of heteroatomic compounds varies between oxygen 0.3–4.9 %, sulfur 0.3–10.3 % and nitrogen 0.6–3.3 %. These molecules also contain thiophene, pyrrole, pyridine, quinoline rings and functional groups such as hydroxyl, carbonyl, carboxyl, sulfide, sulfoxide, and porphyrins containing nickel and vanadium [13–15].

Asphaltenes are compounds characterized by a high degree of aromaticity and polydispersity. The size and complexity of molecules determine solubility. Taking into account these parameters, asphaltenes are soluble in aromatic solvents such as toluene, benzene, and pyridine, but are insoluble in low-boiling paraffins [16–18].

Since the gensis of crude oil depends on a number of factors, the amount and structure of asphaltenes vary in oils obtained from different sources. Several types of structures have been proposed to define the complex asphaltene molecule. The structure of the asphaltene molecule is described by two different models: the continental or “island” model and the archipelago model. In the “island” model proposed by Yen and Mullins, the asphaltene molecule consists of condensed aromatic rings surrounded by an aliphatic chain. In the “archipelago” model proposed by Murgic, the condensed aromatic rings of asphaltene are interconnected by short aliphatic side chains and sometimes by polar bridges [19–22].

Significant differences were found in the chemical structure and properties of asphaltene deposits formed during the transportation, storage and processing of crude oil. Thus, asphaltene samples obtained from stored oils have high polarity, they have more heteroatoms, and less substituted aromatic structures [23].

Due to their structure and composition, asphaltenes tend to form aggregates of different sizes due to numerous intermolecular forces (hydrogen bonds, acid-base, donor–acceptor, dipole–dipole, π-complex exchange, polarization induction forces, van der Waals hydrophobic forces and electrostatic attraction of molecules). Therefore, depending on the amount of asphaltenes in the oil, they can be in the form of molecular states, nanoaggregates and clusters [24–27].

On the other hand, the cause of asphaltene precipitation in oils can be determined by the change in ionization potential and electrical conductivity. Electrical conductivity is an important factor in the explanation of the interaction of asphaltenes with other components of crude oil. The electrical properties of asphaltenes are affected by many parameters such as the origin/composition of crude oil, electrical properties of various components of oil, solvents, pH and electric field voltage [28–32].

Physico-chemical characteristics and structural parameters of separated asphaltenes from crude oils are determined in a complex way by a number of analytical methods (elemental analysis, X-ray diffraction analysis, NMR, UV–Vis and FTIR spectroscopy, mass spectrometry, ICP–MS and SEM). Based on the obtained data, the structural model of the average asphaltene molecule was determined [33–41].

The condensed aromatic hydrocarbons and porphyrins contained in asphaltene were studied by UV–Vis spectrophotometer at a wavelength of 190–1100 nm in different solvents (cyclohexane, acetonitrile and HCO) [42,43]. Aromatic hydrocarbons and their average molecular structures were determined in asphaltenes and tars using FTIR spectroscopy. The infrared spectra of asphaltene and tar were theoretically and practically compared and a linear correlation was obtained [44].

The lack of involvement of other physicochemical analysis methods in the research is one of the drawbacks of the work.

The structure of asphaltene was studied by means of a mass spectrometry under atmospheric pressure and photoionization conditions [45]. In order to identify the main aromatic structures, the dissociation process was carried out by means of infrared multiphoton. In this study, there was no complex approach for the analysis of the structure, and the fragments to describe the structure were not clearly given.

The properties of asphaltenes, including the tar-asphaltenic molecules (TAM) contained in the oils of different regions of Azerbaijan, have been partially studied due to the lack of a perfect scientific-methodical and instrumental-analytical base. These include the offshore oil wells such as Darwin Kupesi, Guneshli, Sangachal, Neft Dasları, and Alat, as well as onshore oil wells such as Yaglı Balakhani, Surakhani, Jafarli, Shikhabi and healing Naftalan [46,47].

TAM structure-group compositions of Darwin Kupesi, Guneshli, and Sangachal oils were studied by proton magnetic resonance and X-ray spectroscopy [48–50]. 80–85 % of the composition of asphaltene molecules consists of carbon atoms that play the role of a framework.

The ratio of carbon to hydrogen (C/H) in the asphaltene molecule of oils obtained from offshore deposits varies in the range of 3.16–3.32. The asphaltenes of Guneshli oil are more crystalline than the asphaltenes of Darwin Kupesi oil. Asphaltenes of oils obtained from the Chirag field are amorphous. In addition, alcohol fragments were found in the asphaltene of Darwin-Kupesi and Guneshli oils, and simple ether bridges were found in the polycycloarene structure of the asphaltene molecule of Jafarli oil. The increase in the degree of aromaticity in the asphaltene component of these oils (Ca = 4.8–5.3) is related to the condensation of individual benzene rings into bi- and polycyclic aromatic structures. Asphaltene molecules of Shikhbi and Alat offshore oils do not contain aliphatic fragments longer than methyl moiety [51].

In asphaltene molecules of these oils, the proportion of carbon ranges from 26-41 % in aromatic structures and 13–68 % in naphthenes. On average, the composition of asphaltene is composed of polycyclic blocks with 2–3 rings. The triarene (phenanthrene) core dominates in the asphaltenes of Darwin-Kupesi and Jafarli oil fields. According to the calculations, polyarene nuclei in asphaltene molecules consist of 3 homo- and heteroaromatic rings (Ka = 2.1–3.1). Each of these polyarene cores (K_{sat} = 2.9–9.7) is united with saturated rings, and the total number of saturated rings in the molecule is K_{sat} = 5.2–12.8. The asphaltene molecules of Sangachal marine oils differ from the asphaltenes of other oils by the presence of a naphthenic ring. There are almost no asphaltenes in the paraffinic oils of Azerbaijan, such as Surakhanı, oily Balakhanı, and Bibiheybat [52].

The method of thermal analysis (TG and DTA) is used to determine the temperature-dependent changes in the physicochemical properties of asphaltenes and to study the amount of coke formed during their pyrolysis. Kinetic studies show that the thermal decomposition of asphaltenes is a first-order reaction and the formation of coke occurs rapidly at temperatures above 499 °C [53,54].

By means of quantum chemical calculations, which have become very relevant in recent times, it is possible to predict the molecular structure of asphaltene based on the study of important parameters such as the bond lengths and angle degrees in the asphaltene molecule, E_{HOMO}, E_{LUMO}, ΔE_{gap}, chemical hardness, chemical softness, electronegativity, chemical potential, electrophilicity index, ionization potential, and electron affinity. [55,56]. Some scientific research conducted partially informs about the chemical composition of asphaltenes in the oils of the sea deposits of Azerbaijan.

Due to the depletion of oil reserves in most of the above-mentioned oil wells, there is a need to process high-yield Zagli crude oil. The lack of information about the amount and structure of the asphaltene component in Zagli oil, which has a sufficient share in Azerbaijan’s oil production, complicates its processing and the purposeful use of the obtained products.

Unlike the previous studies, in the presented research work, for the first time, the average molecular structure, chemical composition, thermal and electrical properties of asphaltene separated from the oil of the onshore Zaglı field of Azerbaijan (AZO) were comprehensively studied, the dimensions of the aggregates were determined in different solvents, and the theoretical calculations of the structure were carried out. The research work was carried out with the complex application of

analytical techniques such as elemental analysis, FTIR, NMR, UB-Vis spectroscopy, XRD, SEM, DLS, and DTA. The methodology is presented in the second section, and the results of the spectroscopic analysis are discussed in the third section.

2. Experimental section

Asphaltenes of Zaglı oil were separated using the standard ASTM procedure, ASTM D6560-12 [57]. First of all, we dissolve 50 g of crude oil in n-heptane at a ratio of 1:40 and keep it in the dark for a day. Then that solution is filtered through Whatman filter paper (brand 42, d = 125) and extracted with heptane until it turns white again, placed in a soxhlet together with the filter paper. At this time, hydrocarbons and tar deposited on asphaltene are cleaned. The sample is dried in an oven at a temperature close to 100 °C in an inert nitrogen atmosphere for 45 min.

Elemental analysis was performed on an American-made Leco Corporation 3000 Lake instrument, model №630-200-200.

The IR-spectrum of the asphaltene sample separated from Zaglı oil was recorded on a zinc-selenide crystal at room temperature in the Alpha Fourier spectrophotometer manufactured by the German company BRUKER in the wave number range of 400–4000 cm^{-1}.

^{1}H NMR, ^{13}C NMR spectra of the studied asphaltene were recorded at 20 °C on a BRUKER-Fourier (300 MHz) spectrometer. Tetramethylsilane (TMS) was used as an internal standard and deuterated chloroform was used as a solvent (concentration: ^{1}H NMR ~ 2 %, ^{13}C NMR ~ 7 %).

To study the electronic structure of asphaltenes, a UV/Vis 6850 spectrophotometer manufactured by JENWAY was used. The operating range of this modern, high-sensitive, dual-beam spectrophotometer is 190–900 nm, and the optical emission of the device is 0.1 nm. Mercury and incandescent lamps are used as excitation sources. The study is performed in a 1 cm quartz cuvette at room temperature. Toluene is used as a solvent and 1 and 0.01 %wt. asphaltene solutions are prepared.

Thermal properties of asphaltene of Zagli oil (TG/DTG/DTA) were determined on a synchronous STA449F3 Jupiter thermoanalyzer (NETZSCH, Germany) in thermoprogrammed dynamic mode, in an inert environment (nitrogen), starting from room temperature, with a temperature increase of 10 °C/min from 23 to 1000 °C temperature range. The inert gas (N_2) flow rate was 20 ml/min, and the amount of sample used was 7–10 mg.

The X-ray phase composition of the asphaltene sample was determined in X-Ray TD-3500 diffractometer (manufactured in China) using a monochromatic set of X-rays (CuKα, α = λ = 1.5406Å) and Ni- filter was taken at room temperature in 2θ = 5-90° angle interval.

An electron scanning microscope Hitachi S-3400 N with an atomic analyzer OXFORD Instruments was used for photomicrographs of the analyzed asphaltene sample.

Asphaltene particle size change analysis was performed by solvent-dependent dynamic light scattering (DLS) (HORIBA LB-550, Japan). The size range is 1–6 μm. Measurements were made at a temperature of 298 K using a laser diode light source with a power of 5 mW at a wavelength of 650 nm. Using three different solvents (octane, xylene, ethanol) for measurements, solutions of the same concentration (0.1 % wt.) were taken, the diffusion coefficients were 1.02, 3.22, and 5.24 m^2/s, respectively. During the DLS measurement, the value of the diffusion coefficient is given by the device depending on the size of the particles.

The entire calculations conducted in the present work were performed at the DFT/B3LYP level in the ORCA-4.2.1 package program with a 6-311G(d,p) basis set.

The physicochemical properties of Zaglı oil are given in Table 1. This heavy oil contains 11.6 and 1.6 % of tar and asphaltene, respectively [57–62].

After purifying Zaglı oil from asphaltenes, it was separated into hydrocarbon content [63–65] by means of liquid adsorption chromatography. The composition of this oil consists of 32.6 % paraffin, 7.9 % naphthene, and 46.3 % aromatic hydrocarbons. 11.6 % by mass of its composition is resin and 1.6 % by mass is asphaltene.

The average molecular mass of asphaltene separated from Zaglı oil was 776, and it was determined by the cryoscopy method in naphthalene solvent. This method is based on measuring the crystallization temperature of asphaltene in the solution by recording the temperature change during the cooling of the asphaltene solution dissolved in naphthalene [66].

3. Results and discussion

The IR-spectrum of asphaltene separated from Zagli crude oil was taken and its functional groups were studied (Fig. 1). The peaks recorded in the spectrum are given in Table 2 [67–69].

It should also be noted that the peak at the 3332 cm^{-1} absorption band corresponds to the stretching vibration of N–H and H-O bonds coincides.

^{1}H and ^{13}C NMR spectra of the investigated asphaltene are shown in Figs. 2 and 3.

In the ^{1}H NMR spectrum of asphaltene, the hydrogen signals of CH_3 groups belonging to the linear or branched alkyl fragment are observed at around 0.91 ppm, which corresponds to the literature data, according to which the mentioned signal is observed at 0.50–1.00 ppm [71–73]. In literature sources [74], the signals related to CH_3 groups attached to the aromatic ring in the α-position are found in the interval of 2.3–2.6 ppm (Fig. 2). On the other hand, signals corresponding to hydrogen atoms of CH– and $–CH_2$ groups attached to the aromatic nucleus are observed in the interval of 2.5–3.5 ppm. If we look at the spectrum of asphaltene, it is possible to say that the signal recorded in the area of 2.2–2.6 ppm corresponds to the CH_3 group attached to the aromatic ring and the signal observed in the 2.6–3.3 ppm interval corresponds to hydrogen atoms belonging to CH– and $–CH_2$ groups attached to the aromatic nucleus. It should also be noted that the CH_2 group attached to the S atom is also observed in the same interval (2.4–3.5 ppm) [75,76]. In the spectra, the signals related to CH_3 and aliphatic CH_2 groups combined in the β-position to the aromatic core are recorded around 1.27 ppm, which corresponds to the literature data, according to which the mentioned signals are observed in intervals of 1.0–1.7 ppm. The signals of hydrogen atoms belonging to β-CH– and CH_2 groups linking to naphthenic hydrocarbons and some hydroaromatic compounds are observed at 1.7 ppm, which also corresponds to the literature data (1.7–1.9 ppm) [77]. In general, the aliphatic hydrogen signals are observed in the interval of 0.5–4.5 ppm [78]. According to the literature source [130], monoaromatic protons in the spectrum are observed in the area of 6.0–7.0 ppm, while the signals related to di-, tri-, and tetra-aromatic protons are recorded in the 7.0–9.1 ppm interval. In addition, the signal recorded at 9.94 ppm corresponds to NH, whereas the signal observed at 11.76 ppm corresponds to the hydrogen atom of the carboxyl group.

The ^{13}C NMR spectrum of the sample was identified based on literature sources [79,80]. The signals recorded at 13.64 and 14.17 ppm belong to the carbon atom of the terminal CH_3 group of the aliphatic chain containing three carbon atoms (Fig. 3). The carbon atoms of the CH_2 group owned by the aliphatic chain and naphthenic ring are observed at 29.76, 23.18, 25.50, 24.62, 25.50, 26.76, 29.20, 29.76, 29.11, 29.73, 30.11, 32.03 and 34.34 ppm. The observed signal at 38.73 ppm refers to the carbon atom combined with sulfur, and the recorded

Table 1
Physico-chemical properties of Zagli oil.

Density, kg/m^3, 20 °C	Kinetic viscosity m^2/s, 20 °C	Quantity of sulfur, %	Ignition temperature ^0C	Freezing temperature, ^0C	Asphaltene, % mass.	Tar, % mass.
847.9	5.0298	0.1588	+9	−30	1.6	11.6

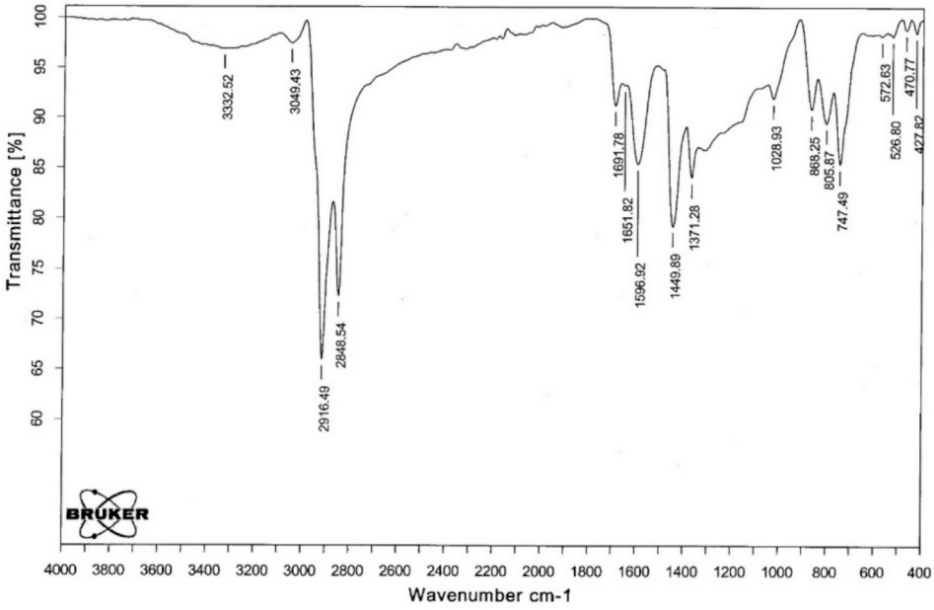

Fig. 1. IR spectrum of asphaltene of Zagli oil.

Table 2
Bands and corresponding chemical bonds observed in the ATR-FTIR spectrum of asphaltene of Zagli oil.

Wavenumber, cm^{-1}	Comments	References
427, 470	stretching vibration of S-S bond (weak)	[68]
572	stretching vibration of S-C bond (weak)	[68]
747, 805, 868	deformation vibration of the C–H bond of the aromatic ring	[67,70]
1028	stretching vibration of the C-O bond of acid	[70,88]
1371, 1449	deformation vibration of the C–H bond of CH_3 and CH_2 groups	[67]
1596	stretching vibration of the C–C bond of the aromatic ring	[69,70]
1651	deformation vibration of N–H bond (weak)	[68]
3332	stretching vibration of N–H bond (weak)	[68]
3332	stretching vibration of the H-O bond of acid	[69]
1691	stretching vibration of the C = O bond of the carbonyl group	[67]
2848, 2916	stretching vibration of the C–H bond of CH_3 and CH_2 groups	[67,69]
3049	stretching vibration of the C–H bond of the aromatic ring	[70]

signal at 53.08 ppm refers to the carbon atom combined with nitrogen. The signals, recorded at 47.74 and 49.22 ppm, correspond to the carbon atoms belonging to the naphthene ring attached to the aromatic nucleus, whereas the signals observed at 73.21 and 81.89 ppm belong to the carbon atoms of the saturated ring connected to the oxygen atom. Signals for carbon atoms belonging to the aromatic core are observed at 115.40, 117.59, 118.59, 121.99, 126.38, 127.38, 128.18, 128.98, 131.17, 132.17, 132.97, 134.57, 137.16 and 138.16 ppm. The signal, recorded at 169.73 ppm, corresponds to the carbon atom of the carboxyl group.

In this section, the structural group analyses were performed based on the results of molecular weight, elemental analysis, ^1H NMR, ^{13}C NMR and FTIR analysis. Structure-group analyses were calculated based on available literature sources [80–85]. The amount of C, H, N, S, and O elements of asphaltene was determined by the method of elemental analysis, according to which the following was found: C 75.6 %, H 7.0 %, O 6.2 %, N 1.7 %, S 8.1 %.

The results obtained from elemental analysis and molecular weight

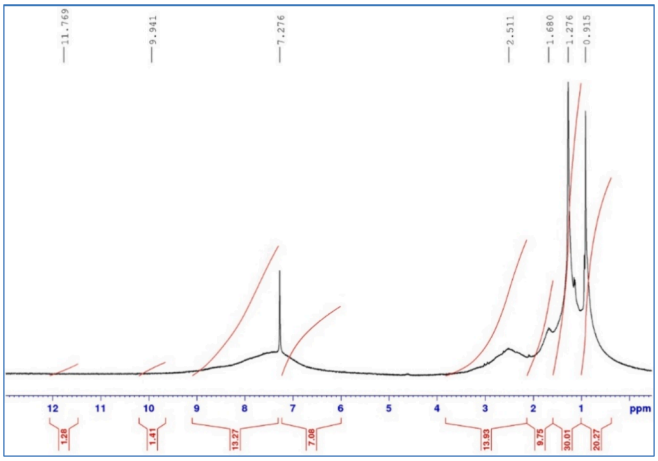

Fig. 2. ^1H NMR spectrum of asphaltene of Zagli oil.

were used to determine the chemical structure of asphaltene.

The numbers of other atoms were found in the same way: C- 49.50, H- 55.00, O- 3.04, N- 0.95, S- 2.00. Comparing the number of elements, it can be seen that the number of oxygen in the asphaltene molecule is more than other heteroatoms. Based on the results of the calculations, the empirical formula of the investigated asphaltene can be written as $C_{49.5}H_{55}O_{3.04}N_{0.95}S_2$.

The relative distribution of hydrogen by structural groups in the ^1H NMR spectrum was calculated based on integral ratios. The structural-group parameters of the studied asphaltene are given in Table 3.

Comparing the relative distribution of hydrogens [79] shows that the main difference is in the relative share of H_p and H_{ar} hydrogens. Thus, the relative share of hydrogens belonging to the paraffin fragment is about 10 % more, and the relative share of hydrogens belonging to the aromatic fragment is about 9 % less. There is no significant difference in the relative distribution of hydrogen atoms belonging to the H_α and H_γ fragments.

According to the results of IR, NMR, elemental analysis and structure-group analysis, the approximate molecular structure of the investigated asphaltene can be described in two ways:

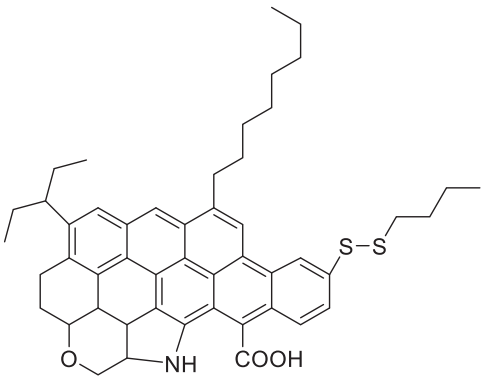

As1

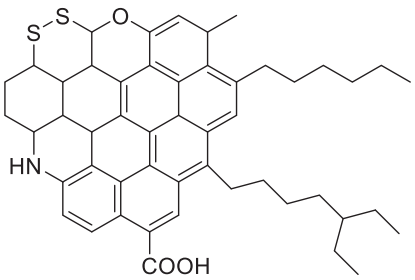

As2

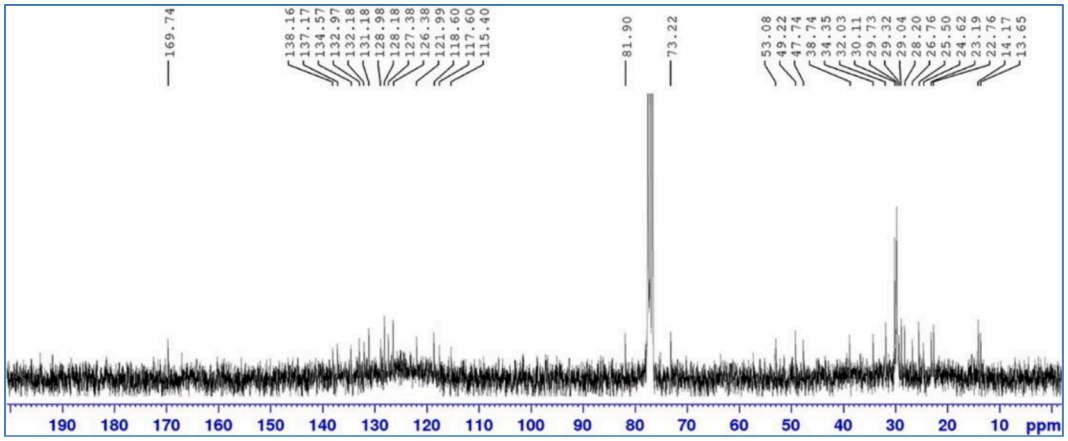

Fig. 3. ^{13}C NMR spectrum of asphaltene of Zagli oil.

Table 3
Structural-group parameters of asphaltene of Zagli oil. Relative distribution and number of hydrogen atoms (H_α, H_n, H_p, H_γ, H_{ar}, NH, COOH, f_{ar}), number of rings (R_t, R_{ar}, R_s), number of carbon atoms (C_α, C_n, C_p, C_γ, C_{ar}, COOH).

Relative distribution of hydrogen (%)							
H_α	H_n	H_p	H_γ	H_{ar}	NH	COOH	f_{ar}
13.93	9.75	30.01	20.27	20.35	1.41	1.28	0.53
The number of hydrogen atoms							
7.7	5.4	16.5	11.1	12.8	0.8	0.7	
The number of rings			The number of carbon atoms				

R_t	R_{ar}	R_s	C_α	C_n	C_p	C_γ	C_{ar}	COOH
10.1	5.9	3.7	3.8	6.7	8.6	3.7	25.7	1.0

H_α – hydrogen atoms attached to the aromatic ring in the α position;
H_n – hydrogen atoms belonging to the naphthenic fragment;
H_p – hydrogen atoms belonging to the paraffin fragment;
H_γ – hydrogen atoms belonging to terminal methyl groups;
H_{ar} – hydrogen atoms belonging to the aromatic nucleus;
f_{ar} – degree of aromaticity.
R_t – total number of rings;
R_{ar} – the number of aromatic rings;
R_s – the number of saturated rings;
C_α – the number of carbon atoms bonded to the aromatic ring in the α position;
C_n – number of carbon atoms belonging to saturated rings;
C_p – the number of carbon atoms belonging to the paraffin fragment;
C_γ – the number of carbon atoms belonging to the terminal methyl groups;
C_{ar} – the number of carbon atoms belonging to the aromatic nucleus.
C_{hc}– the number of carbons belonging to a hydrocarbon fragment.

Comparing the proposed structures with the results of structural group analysis, we see that the number of heteroatoms (N, S, O) is the same. According to the results of the analysis, there are 3.7 terminal methyl groups. There are 4 terminal methyl groups in As1 and 3 in As2. The number of aromatic rings is the same in the analysis results (5.9) and in the proposed structures (6). As1 and As2 have 24 aromatic carbon atoms, which is close to the results of the analysis (25.7). The presence of some discrepancy in the saturated fragments can be explained by the shifting of the carbon and hydrogen signals attached to the heteroatoms towards the weak area in the spectrum. As1 compound has 7 carbon atoms attached to heteroatoms. The other 42 carbon atoms belong to the hydrocarbon fragment (C_{hc}), which is confirmed in equation 8 (C_{hc} = 41.7). Thus, as a general result of the structural-group analysis, it can be noted that the average molecular structure of the studied asphaltene has a total of 49.5 carbon and 55 hydrogen atoms. The aliphatic chain (C_α, C_p, C_γ) has only 16.1 number of carbon atoms. The number of total rings is 10.1, the number of saturated rings is 4.2, and the number of aromatic rings is 5.9. The number of carbon atoms in the naphthenic fragment is 6.7, and 25.7 in the aromatic fragment.

As a result of the spectroscopic studies, it can be assumed that the average molecular structure of the asphaltene sample separated from Zagli oil corresponds to the continental model [24,25].

The X-ray diffraction method was used to fundamentally study the structure of asphaltenes. As a result of X-ray diffraction analysis of the asphaltene sample of Zagli oil, peaks at 2θ → 21.394°, 23.818°, 31.613°, 39.211° angles are observed in the diffractogram (Fig. 4), which represents the scattering pattern of both phases, viz the amorphous and crystalline, of the asphaltene sample. The angle 2θ = 21.394° appearing in the γ band in the spectrum belongs to the aliphatic part, and 2θ = 23.818° in the graphene band belongs to the aromatic part. The third diffraction peak associated with the aromatic layers of asphaltenes is observed at 2θ = 39.211°. The presence of crystal planes in the radiograph of petroleum asphaltene is indicated by straight lines.

Petroleum asphaltenes give diffraction of X-ray reflection similar to amorphous substances, and since the composition and quantity of the crystalline phase are small, the boundary of this phase can be marked with a straight line in the diffractogram [86,87].

Thus, the presented data allow us to make certain recommendations in the study of the amorphous-crystalline phase composition of carbonaceous materials without diamond-like structures.

Three asphaltene solutions with different concentrations were used to clearly obtain the UV–Vis spectra of the complex asphaltene compound.

Since more energy is required for electron transitions of saturated substances, their absorption bands are not recorded in the UV–Vis spectral range (Fig. 5).

Absorption peaks of aromatic hydrocarbons are observed in this spectral region, and as the number of rings in these compounds increases, a shift towards the red region occurs [88–90]. The asphaltene solution concentration was reduced to obtain narrower wave peaks.

In the UV spectrum, the broad complex band of the asphaltene molecule in the wavelength range of 200–300 nm can be attributed to the presence of aromatic hydrocarbons. As it can be seen from the spectra, the peaks of the individual absorption bands of all aromatic components overlap. Thus, the absorption peaks recorded in the spectral range of 200–250 nm are mainly related to the δ-π * transition and the absorption bands of 260, 279 nm are related to the π-π * transition. In the spectrum, the Soret band corresponding to the Alg → Eu transition is observed at a wavelength of 401 nm and is ascribed to vanadium porphine. In porphyrins, these absorption bands result from electronic transitions between HOMO and LUMO. The HOMOs were calculated as Alg orbitals and the LUMOs as a degenerate set of Eu orbitals. The predominance of vanadium porphine in the composition of AZO distinguishes it from other oils [91,92].

Fig. 6 (a and b) shows photomicrographs of asphaltene of Zagli oil analyzed by scanning electron microscope. A less porous surface is observed in Fig. 6 (a). Agglomerates of various shapes and sizes are suitable for asphaltenes. SEM photomicrographs of asphaltenes show that the upper surface of the agglomerates are brittle solids. The picture shows the scaly surface of the asphaltene and unevenly distributed voids on the surface. Tar separation causes voids in the asphaltene layers. Asphaltene aggregates consist of particles with a size of 800 μm [93–95].

In the lower part of Fig. 6 (a), reticular bands are visible, indicating the crystal boundaries of the stacked layers. According to SEM figures, it is possible to suggest that the aggregates are particles with a Lamellar structure. The element composition of asphaltene particles was analyzed by energy dispersive X-ray spectroscopy (EDX) combined with SEM, and the elements observed in the sample according to the spectrum are shown in Table 4.

All metals contained in oil are concentrated in tars and asphaltenes.

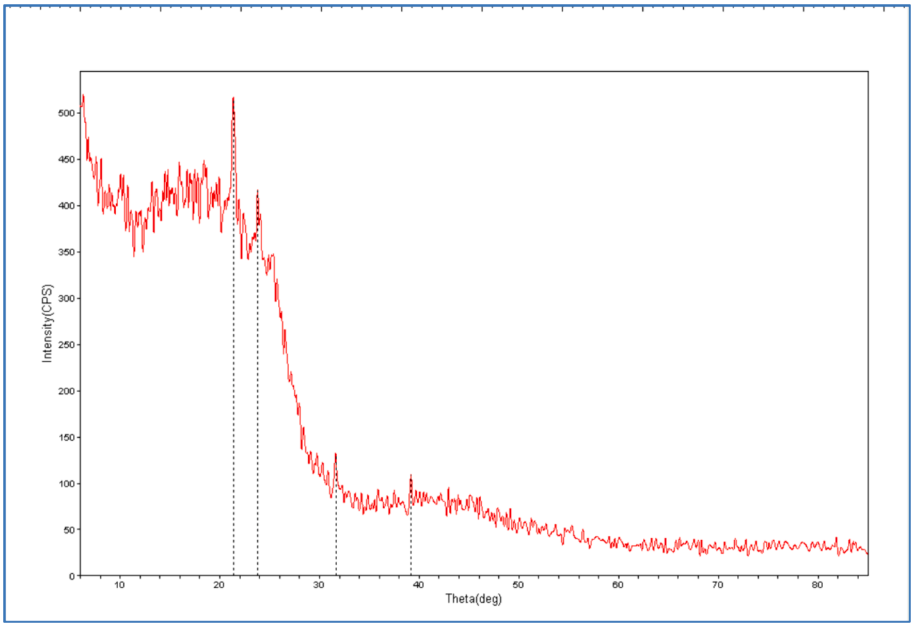

Fig. 4. X-ray phase rentgenogram of asphaltene sample.

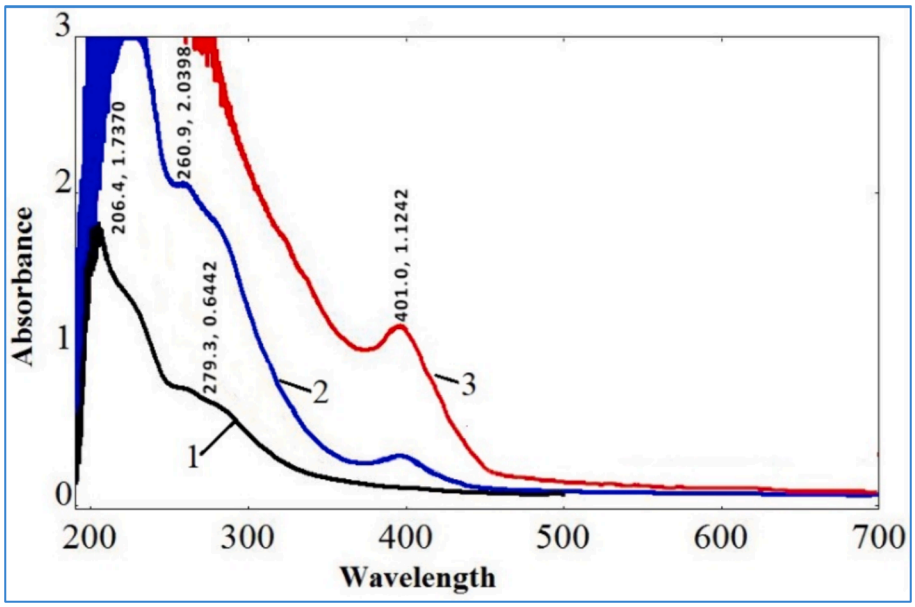

Fig. 5. Electronic absorption spectra of petroleum asphaltene in different concentrations, %wt.: 1—0.01; 2—0.1; 3—1

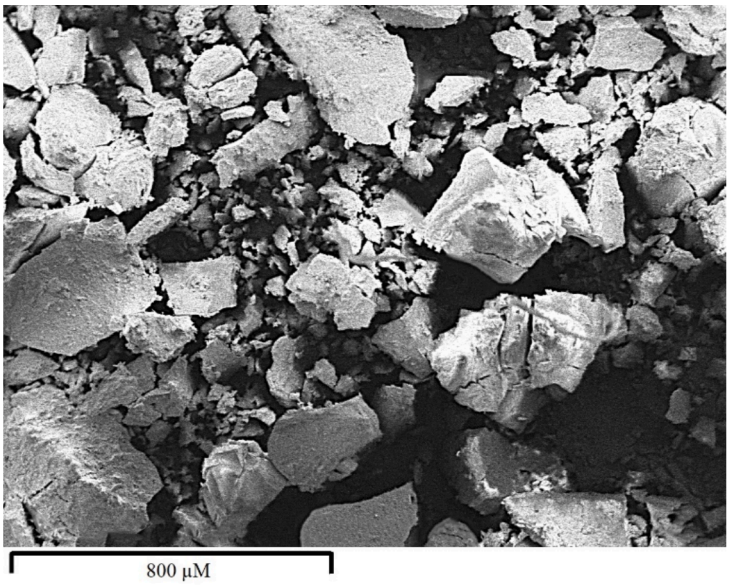

a)

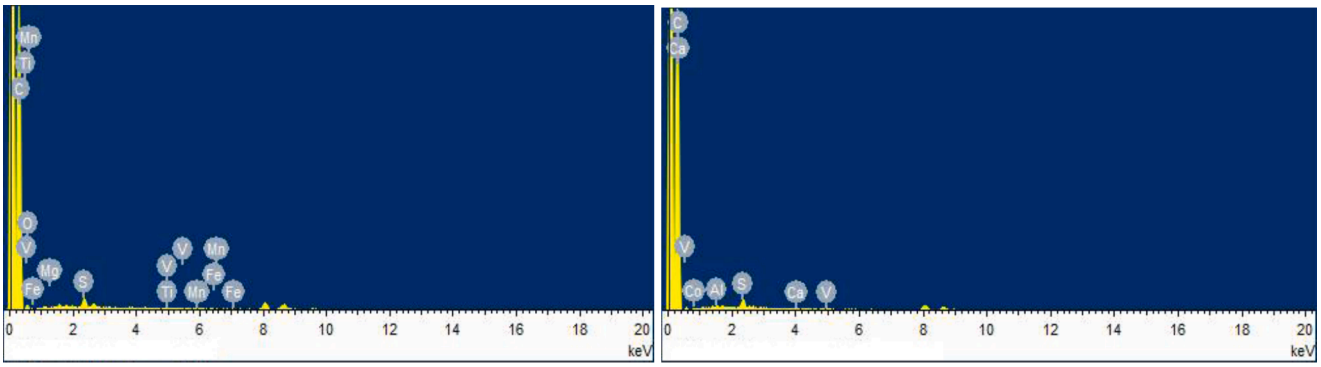

b)

Fig. 6. SEM photomicrographs of asphaltene of Zagli oil (a), energy dispersive X-ray spectroscopy (EDX) data combined with SEM (b).

Table 4
Metals contained in the asphaltene of Zagli oil.

Metal composition of asphaltene	V	Ni	Fe	Ca	Co	Na	Mn	Ti	Al	Mg
Amount, %	0.06	0.01	0.06	0.01	0.03	0.02	0.04	0.05	0.19	0.02

Although asphaltenes have an amorphous structure, their semiconducting properties are associated with π electrons. Thus, dielectric (paraffin, naphthenic and aromatic hydrocarbons) and semiconducting (polycyclic aromatic hydrocarbons and porphyrins) components interact with each other in asphaltene. For this reason, their energetic electronic spectra and properties of electrons correspond to the properties of crystalline semiconductors. In order to determine the electrical properties of asphaltenes, in particular, the charge transfer mechanism, it is necessary to study their electronic structure, as well as the degree of interaction with each other and with surrounding hydrocarbon molecules [96,97].

Donor-acceptor properties were studied based on electronic absorption spectra in 0.1 g/l asphaltene toluene solution. The ionization potential (I) and electronegativity (A) of asphaltenes were calculated according to the integral characteristic – the area of the broadband signal, the so-called integral oscillator power (ISO). To determine the semiconducting nature of petroleum asphaltenes, it is necessary to study its electrical conductivity. At room temperature, their electrical conductivity is 10^{-14} – 10^{-11} $\Omega^{-1}m^{-1}$ and the increase in electrical conductivity is associated with paramagnetic centers [98–100].

The value of I is 5.16 eV and the value of A is 2.21 eV. As a result of the research conducted in the UV–visible field for asphaltenes, the presence of low I and high value for A indicates that the molecule is electrically conductive and has donor–acceptor properties.

Measurements were carried out in an alternating current source at a frequency of 1kHs, using a two-contact method, through an E7-20 bridge, solid state. The specific electrical conductivity of the investigated asphaltene at a temperature of 25 °C is $2.42\bullet10^{-11}$ $\Omega^{-1}m^{-1}$, and its specific resistance is $4.14\bullet10^{10}$ Ω•m. Then, the specific electrical conductivity and resistance of the sample at different temperatures were looked at and shown in Table 5.

It can be seen from Table 5 that an increase in temperature up to 100 ℃ causes a relative increase in specific resistance and specific electrical conductivity of the studied asphaltene sample. However, it behaves like a dielectric in the temperature range of 25–100 ℃. The reason for this is that free radicals are not formed due to the strong carbon bonds. In this temperature interval, the value of specific electrical conductivity varies in the range $\rho = 10^{-11}$-10^{-10}.

According to the thermal analysis performed on AZO, physical processes such as softening and liquefaction of the sample occur in the TG/DTG curve as the temperature rises from 23 °C. Usually, structural phase transitions leading to changes in the size and activity of molecular aggregates of asphaltenes begin at temperatures around 36–38 °C, and a "critical" temperature is reached in this temperature range (Fig. 7) [56,101]. At this time, depending on the structure-composition of the studied asphaltene, molecules, that are weakly connected to the surface and turned into a light gas, move from one surface to another surface. These molecules are located in the spaces between the layers, and in connection with this, a relative increase in volume is observed.

Table 5
Temperature dependence of specific electrical conductivity and specific resistance of asphaltene molecule.

Temperature, °C	Specific electrical conductivity, $\Omega^{-1}m^{-1}$	Specific resistance, Ω•m	Resistance, Ω
25	$2.42\bullet10^{-11}$	$4.14\bullet10^{10}$	$6.53\bullet10^{8}$
50	$4.76\bullet10^{-11}$	$2.1\bullet10^{10}$	$3.3\bullet10^{8}$
75	$6.2\bullet10^{-11}$	$1.61\bullet10^{10}$	$2.25\bullet10^{8}$
100	$1.16\bullet10^{-10}$	$8.6\bullet10^{9}$	$1.35\bullet10^{8}$

Up to 406 °C, the asphaltene sample is thermostable, does not undergo thermochemical conversion, and its mass decreases by 0.09 %. In the conducted research works of Karacan et al. and Boytsova et al. [102] it was reported about the distillation of alkane and low molecular weight aromatic compounds at the temperature of 100–300 °C and it was mentioned that the degradation of tars started at 200 °C. However, the reason for such a decrease in mass in the temperature range of 23–406 °C is the evaporation of the solvent remaining in the asphaltene sample of Zagli oil after extraction or the breaking of aliphatic side chains (α-methyl and α-methine moieties).

A three-stage thermochemical process is observed in AZO at temperatures higher than 406 °C. In the initial stage of pyrolysis, in the temperature range of 406–505 °C, the mass of the sample decreases by 14.63 %. It is assumed that at this stage of pyrolysis, high-molecular compounds are degraded: mainly, the breaking of large-molecular alkyl bonds and sulfur bridges takes place (Fig. 7).

The exothermic peak (505 °C) observed in the temperature range of 454–599 °C is probably related to the condensation reaction. Most likely, this process is related to the oxygen content of asphaltene. In the high temperature range of 505–818 °C, several stages of pyrolysis occur and the mass loss is 72.24 %. Thus, the mass reduction due to thermodegradation of the asphaltene sample in the temperature ranges of 505–638 °C and 638–818 °C is 37.34 and 34.90 %, respectively. This stage of pyrolysis can be associated with polycondensation and coking. After the process is finished, the amount of residual coke is 12.58 %. The two observed endothermic peaks can be related to the cracking process at the phase transitions (Fig. 7).

The thermal property also depends on the thermal decomposition of unstable bonds of heteroatoms (N, S, O and metals) with carbon. The stability of crystallites in a wide temperature range can be explained by the formation of π-π type donor–acceptor complexes.

Therefore, TG and DTG data show that the asphaltene molecule is stable up to 406 °C temperature. In this compound, a 3-stage pyrolysis process takes place in the temperature range of 406–818 °C and ends with the formation of coke. Endothermic peaks may be related to degradation reactions, while exothermic peaks may be related to internal oxidation or condensation.

At the same time, the diameters of AZO aggregates were studied using measurements of dynamic and static light scattering. This study was carried out on a solution consisting of three different solvents (octane, xylene and ethanol) of the same concentration (0.1 %wt.). The result of the distribution of asphaltene particles (D) in given solvents is shown in Fig. 8.

Fig. 8 shows the corresponding peaks of asphaltene particles soluble in octane, ethanol, and xylene. Thus, the diameter of the aggregates in the xylene solution is 21 nm, the monodispersity increases by 2 times compared to the ethanol solution, and 5 times compared to the octane solution. In ethanol, the particle size increases (76 nm), but its monodispersity decreases. Two peaks were observed in asphaltene aggregates in octane solution. Peak I is at 9 nm, peak II is at 100 nm. The first peak corresponds to the small cluster and the second peak to the large aggregates. The decrease in monodispersity with increasing particle size can be explained by the polarity of the solvent. That is why, with the increase in the diameter of the aggregates, their polydispersity also increases [95,103,104].

Therefore, the size of the aggregates increases as a result of the interaction of the aromatic nuclei of asphaltenes in the octane solution. The hydrogen bonds, formed by the interaction of asphaltene with the solvent (ethanol), lead to the formation of stable aggregates. In xylene,

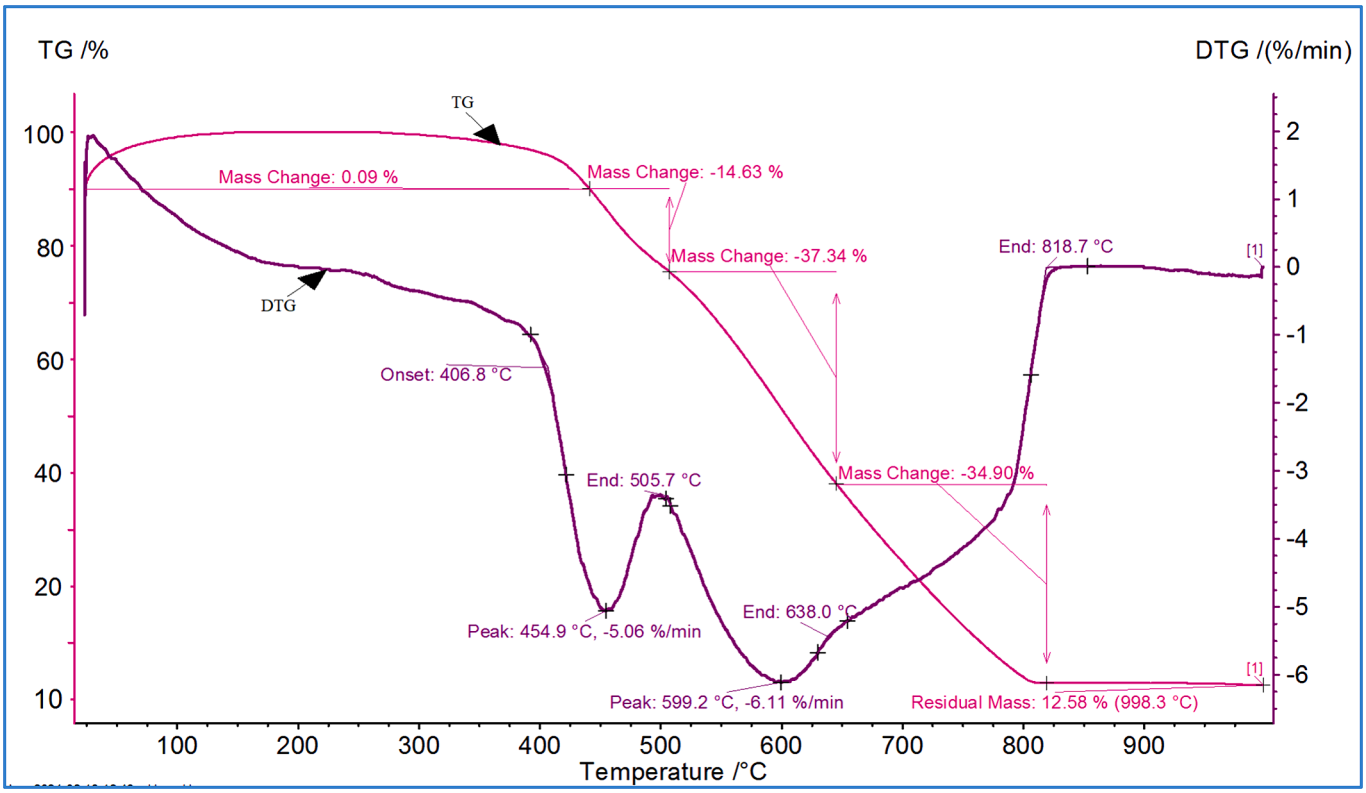

Fig. 7. DTG-TG curve of asphaltene of Zagli oil.

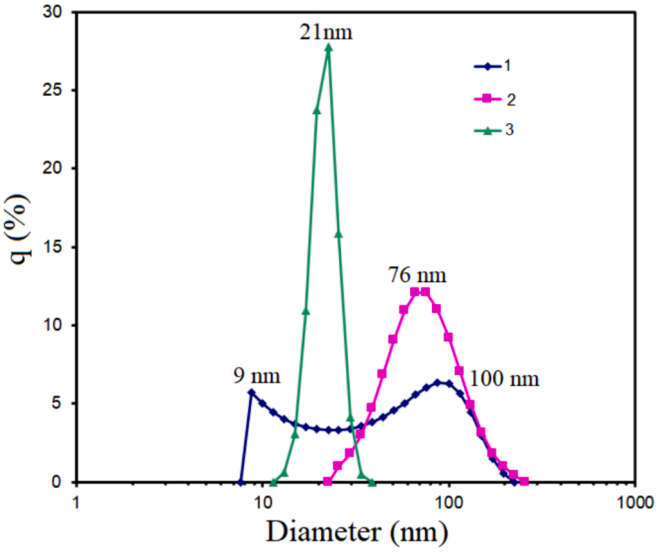

Fig. 8. Results of DLS analyzes of asphaltene aggregates of Zagli oil in different solvents of the same concentration: 1- octane, 2- ethanol, 3- xylene.

the π-π interaction between the aromatic ring of asphaltenes and the aromatic core of xylene causes deaggregation and monodispersity increases. In general, the molecular architecture of asphaltenes (eg, the number and length of chains), the number and position of heteroatoms, and the number and size of aromatic nuclei are the main factors affecting aggregation behaviour. Thus, they all represent the aggregation behaviour of asphaltenes [105,106].

Theoretical calculations of the proposed structures (As1, As2) were performed using the Density Functional Theory (DFT) method, important parameters such as E_{HOMO}, E_{LUMO}, chemical hardness (η), chemical softness (σ), electronegativity (λ), chemical potential (μ), electrophilicity index (ω), ionization potential (I) and electron affinity (A) were studied based on literature sources [107–109]. The optimized structures are shown in Fig. 9.

Based on the optimized structure, it was determined that the longest bond (2.0832 Å) in compound As1 is between S-S. Interestingly, the length of the C-S bonds in the molecule is different. Thus, while the C38-S2 bond length is 1.8444 Å, the C27-S1 bond length is 1.7954 Å. This is because the aromatic nucleus attracts S1 towards itself. The same situation is observed in N-C bonds. The length of the N-C19 bond (1.4673 Å) is shorter than the N-C12 bond (1.5007 Å) due to the attraction of the electron density of the aromatic core. The smallest angle degree (97.8849°) is the C12-C11-C14 angle, where (N-C12-C11-C14) 41.9576° torsion is observed. Another noteworthy point is the observation of −95.7101° torsion in bonds C27-S1-S2-C38.

In the As2 molecule, the C4-C7-S1 (111.9965°) and the C3-C19-S2 angles (114.4674°) are different. This is because oxygen (O1) attracts C19 towards itself with a bond length of 1.4143 Å. There is a small difference (0.0042 Å) in the length of the C-S bonds (S2-C19 and S1-C7). The longest bond (2.0897 Å) in the As2 molecule is the S-S bond. The smallest angle degree (96.5542°) is the angle S1-S2-C19. In this molecule, it is noteworthy that the sulfur atoms break the plane. 68.6476° torsion is observed in the S2-S1-C7-C4 connection, and 60.9619 in the S1-S2-C19-C3 connection. Other bond lengths and angle degrees in As1 and As2 molecules are close (Table S1-S2, ESI). In both molecules, the lowest value of partial charge (−0.477) was recorded in the O3 atom. HOMO (highest occupied molecular orbital) and LUMO (lowest unoccupied molecular orbital) orbitals of both described molecules are given in Fig. 10:

As can be seen from Fig. 10, the HOMO and LUMO orbitals in both molecules are mainly delocalized over the aromatic fragments. Compared to As1, the HOMO orbitals in As2 are expanded towards the alkyl chain. Thus, the HOMO orbitals are delocalized over C23, C31 and C37. It is also observed that the HOMO orbitals in As2 cover oxygen (O1)

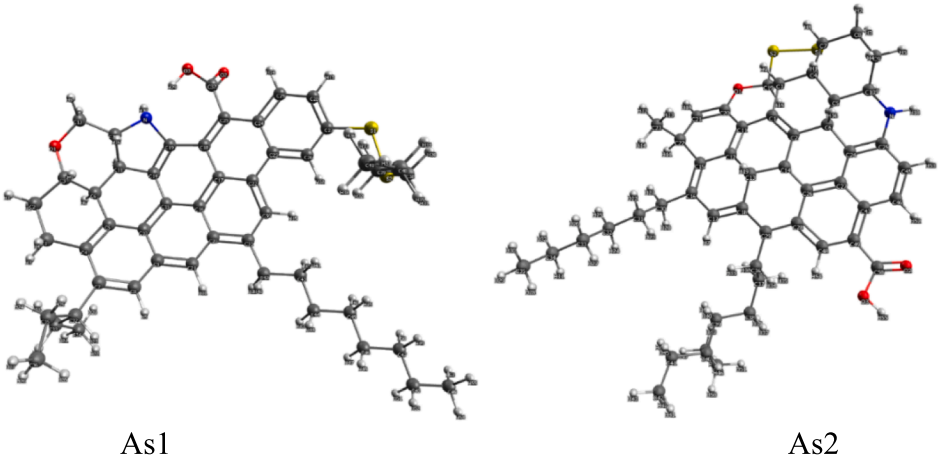

Fig. 9. Optimized structures of the described compounds (As1, As2).

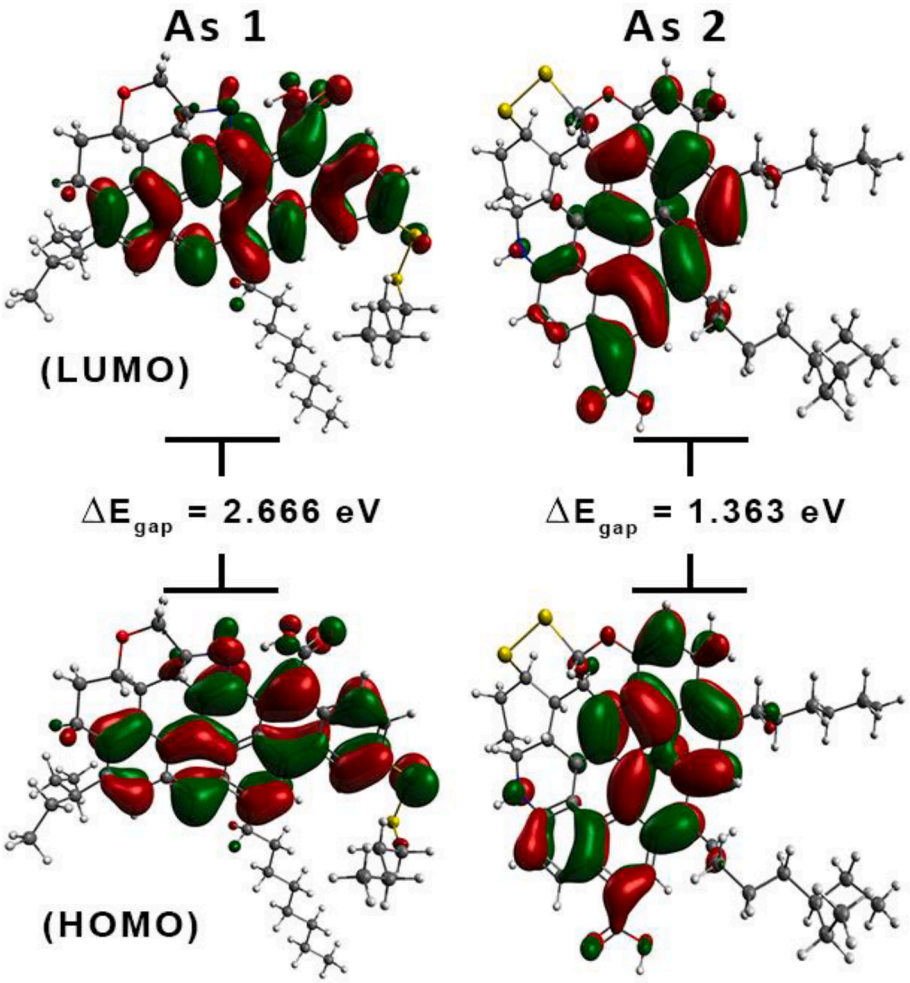

Fig. 10. HOMO-LUMO energy level diagrams for As1 and As2.

in the ring. In As1, unlike As2, HOMO and LUMO orbitals (more HOMO) are delocalized over S1.

Important quantum-chemical parameters (HOMO-LUMO energy gap, single point energy, electronegativity, electrophilic index, ionization potential, electron affinity, and chemical hardness and softness) were calculated and listed in Table 6.

As can be seen from Table 6, single point energies of molecules (As1, As2) are close. ΔE of As1 is about twice as large as ΔE of As2. This difference indicates that As1 is more stable. Thus, a large value of ΔE indicates that the molecule has high stability and low reactivity. Stable molecules become solids. As2 has more softness. In compounds, electronegativity, chemical potential and ionization potential are not very different. Electronegativity (λ) is related to electron attraction. As1 has slightly more electronegativity (3.707) than As2 (3.509). The negative

Table 6
HOMO-LUMO energy gap, single point energy, electronegativity, electrophilic index, ionization potential, electron affinity, and chemical hardness and softness values for As1 and As1.

Compound	As1	As2
Single point energy (Eh)	−2973.917	−3011.917
E_{HOMO} (eV)	−5.040	−4.191
E_{LUMO} (eV)	−2.374	−2.828
ΔE (eV)	2.666	1.363
Chemical hardness, (η), (eV)	1.333	0.681
Chemical softness (σ), (eV)	0.750	1.468
Electronegativity (λ), (eV)	3.707	3.509
Chemical potential (μ), (eV)	−3.707	−3.509
Electrophilicity index (ω), (eV)	5.154	9.034
İonization potential (I), (eV)	5.040	4.191
Electron affinity (A), (eV)	2.374	2.828

chemical potential indicates that molecules do not undergo decomposition into elements [110–112]. It can be seen from Table 6 that As2 (9.034) is almost 2 times stronger electrophile than As1 (5.154). Ionization potential (I) is the energy required to remove an electron. On the other hand, a high value of ionization energy indicates chemical stability. Electron affinity (A) is the energy released when an electron is attached. The ionization potential (5.040 eV) and electron affinity (2.374 eV) of As1 are close to the results of UV analysis (I = 5.16 eV, A = 2.21 eV). If we summarize the above, As1 is more suitable among possible structures.

4. Conclusion

For the first time, the obtained results of the research on the average molecular structure, chemical composition, morphology, thermal and electrical properties, and solubility characteristics in various solvents of asphaltenes isolated from crude oil of Azerbaijan (Zaglı field) using spectroscopic analysis (such as FTIR, NMR, UV–Vis, XRD, SEM, DLS, DTA and DFT) and computational chemistry methods are the following:

The predominance of island structure models consisting of –COOH functional group, C-S, N–H, and −S-S- connected side alkyl chains, condensed ~ 4 naphthenic and ~ 6 aromatic ring molecules was determined in asphaltene content;

The characteristic absorption bands of naphthene-aromatic hydrocarbons (206, 260, 279 nm) and vanadium porphyrin (401 nm) were observed in the UV–Vis spectrum;

Low ionization potential (5.16 eV) of asphaltene and high (2.21 eV) electron affinity are due to the electrically conductive and donor–acceptor properties of its molecule;

The asphaltene compound is amorphous, its composition consists of thin crystalline aggregates with lamellar morphology;

TG and DTG curves show that 12.58 % of coke is formed during the three-stage pyrolysis process of asphaltene, which is thermostable at 406 ℃ temperature, covering the temperature range of 406–818 ℃;

Depending on the polarity of the solvent, the growth of asphaltene particles leads to polydispersity;

According to theoretical calculations, the HOMO-LUMO energy gap value of 2.666 eV demonstrates that the asphaltene compound has high stability and weak reactivity. The agreement of the theoretical calculations of one of the two structures (As1) of asphaltene with experimental results (UV–Vis spectral analysis) indicates that the structure of asphaltene is close to As1.

This knowledge gained about the structure and properties of asphaltenes can be used to prevent problems caused by precipitation and aggregation of asphaltenes in the oil refining process.

CRediT authorship contribution statement

Ulviyya Jeyhun Yolchuyeva: Writing – original draft, Resources, Project administration, Methodology, Investigation, Formal analysis. **Vagif M. Abbasov:** Supervision, Funding acquisition. **Rana Jafarova:** Supervision. **Ayaz Mammadov:** Software, Formal analysis, Data curation. **Saida Ahmadbayova:** Formal analysis. **Ravan A. Rahimov:** Writing – review & editing, Data curation. **Alakbar Huseynzada:** Writing – review & editing. **Fargana Alizadeh:** Writing – review & editing, Validation.

Declaration of competing interest

The authors declare that they have no known competing financial interests or personal relationships that could have appeared to influence the work reported in this paper.

Data availability

The authors do not have permission to share data.

Appendix A. Supplementary data

Supplementary data to this article can be found online at https://doi.org/10.1016/j.fuel.2024.132084.

References

[1] Rogel E, Ovalles C, Vien J, Moir M. Asphaltene characterization of paraffinic crude oils. Fuel 2016;178:71–6. https://doi.org/10.1016/j.fuel.2016.03.030.
[2] Savel'Ev V, Golovko A, Gorbunova L, Kamyanov V, Galvalizi C. High-sulfurous Argentinian asphaltites and their thermal liquefaction products. Oil Gas Sci Technol 2008;63(1):57–67. https://doi.org/10.2516/ogst:2007085.
[3] Mahdavi S, Moghadam AM. Critical review of underlying mechanisms of interactions of asphaltenes with oil and aqueous phases in the presence of ions. Energy Fuels 2021;35(23):19211–47. https://doi.org/10.1021/acs.energyfuels.1c02270.
[4] Dickakian GB, Seay S. Asphaltene precipitation primary crude exchanger fouling mechanism. Oil & Gas Science Technology 1988;86:47–50.
[5] Wang J, Buckley JS, Creek JL. Asphaltene deposition on metallic surfaces. J Dispers Sci Technol 2004;25(3):287–98. https://doi.org/10.1081/DIS-120037697.
[6] Langevin D, Argillier JF. Interfacial behavior of asphaltenes. Adv Colloid Interface Sci 2016;233:83–93. https://doi.org/10.1016/j.cis.2015.10.005.
[7] Alimohammadi S, Zendehboudi S, James L. A comprehensive review of asphaltene deposition in petroleum reservoirs: Theory, challenges and tips. Fuel 2019;252(1):753–91. https://doi.org/10.1016/j.fuel.2019.03.016.
[8] Gaweł B, Eftekhardadkhah M, Øye G. Elemental composition and fourier transform infrared spectroscopy analysis of crude oils and their fractions. Energy Fuel 2014;28(2):997–1003. https://doi.org/10.1021/ef402286y.
[9] Fergoug T, Bouhadda Y. Determination of Hassi Messaoud asphaltene aromatic structure from ^{1}H & ^{13}C NMR analysis. Fuel 2014;115:521–6. https://doi.org/10.1016/j.fuel.2013.07.055.
[10] Bouhadda Y, Bormann D, Sheu E, Bendedouch D, Krallafa A, Daaou M. Characterization of Algerian Hassi-Messaoud asphaltene structure using Raman spectrometry and X-ray diffraction. Fuel 2007;86:1855–64. https://doi.org/10.1016/j.fuel.2006.12.006.
[11] Gao YY, Shen BX, Liu JC. Distribution of nickel and vanadium in venezuela crude oil. Pet Sci Technol 2013;31(5):509–15. https://doi.org/10.1080/10916466.2011.576363.
[12] Mullins OC. The asphaltenes. Annu Rev Anal Chem 2011;4(1):393–418. https://doi.org/10.1146/annurev-anchem-061010-113849.
[13] Yakubov MR, Milordov DV, Yakubova SG, Borisov DN, Ivanov VT, Sinyashin KO. Concentrations of vanadium and nickel and their ratio in heavy oil asphaltenes. Pet Chem 2016;56(1):16–20. https://doi.org/10.1134/S0965544116010072.
[14] Biktagirov T, Gafurov M, Mamin G, Gracheva I, Galukhin A, Orlinskii S. In situ identification of various structural features of vanadyl porphyrins in crude oil by high-field (3.4 t) electron– nuclear double resonance spectroscopy combined with density functional theory calculations. Energy Fuel 2017;31(2):1243–9. https://doi.org/10.1021/acs.energyfuels.6b02494.
[15] Fakher S, Ahdaya M, Elturki M, Imqam A. Critical review of asphaltene properties and factors impacting its stability in crude oil. J Pet Explor Prod Technol 2020;10(3):1183–200. https://doi.org/10.1007/s13202-019-00811-5.
[16] Eyssautier J, Levitz P, Espinat D, Jestin J, Gummel J, Grillo I, et al. Insight into Asphaltene Nanoaggregate Structure Inferred by Small Angle Neutron and X-ray Scattering. J Phys Chem B 2011;115(21):6827–37. https://doi.org/10.1021/jp111468d.
[17] Teklebrhan RB, Ge L, Bhattacharjee S, Xu Z, Sjöblom J. Probing Structure – Nanoaggregation Relations of Polyaromatic Surfactants: A Molecular Dynamics Simulation and Dynamic Light Scattering Study. J Phys Chem B 2012;116(20):5907–18. https://doi.org/10.1021/jp3010184.
[18] Liu J, Zhao Y, Ren S. Molecular dynamics simulation of self-aggregation of asphaltenes at an oil/water interface: Formation and destruction of the

asphaltene protective film. Energy Fuels 2015;29(2):1233–42. https://doi.org/10.1021/ef5019737.
[19] Lin Y, Cao T, Chaćon-Patiño ML, Rowland SM, Rodgers RP, Yen A, Biswal SL. Microfluidic study of the deposition dynamics of asphaltene subfractions Enriched with Island and Archipelago Motifs. Energy Fuels 2019;33(3):1882–91. https://doi.org/10.1021/acs.energyfuels.8b03835.
[20] Priyanto S, Mansoori GA, Suwono A. Measurement of property relationships of nano-structure micelles and coacervates of asphaltene in a pure solvent. Chem Eng Sci 2001;56(24):6933–9. https://doi.org/10.1016/S0009-2509(01)00337-2.
[21] Hemmati-Sarapardeh A, Ameli F, Ahmadi M, Dabir B, Mohammadi A, Esfahanizadeh L. Effect of asphaltene structure on its aggregation behavior in toluene-normal alkane mixtures. J Mol Struct 2020;1220:12860–5. https://doi.org/10.1016/j.molstruc.2020.128605.
[22] Dutta Majumdar R, Gerken M, Mikula R, Hazendonk P. Validation of the Yen-Mullins model of Athabasca oil-sands asphaltenes using solution-state 1H NMR relaxation and 2D HSQC spectroscopy. Energy Fuel 2013;27(11):6528–37. https://doi.org/10.1021/ef401412w.
[23] Daaou M, Larbi A, Martínez-Haya B, Rogalski M. A Comparative study of the chemical structure of asphaltenes from Algerian petroleum collected at different stages of extraction and processing. J Pet Sci Eng 2016;138:50–6. https://doi.org/10.1016/j.petrol.2015.11.040.
[24] Ghosh AK, Chaudhuri P, Kumar B, Panja SS. Review on aggregation of asphaltene visavis spectroscopic studies. Fuel 2016;185:541–54. https://doi.org/10.1016/J.FUEL.2016.08.031.
[25] Evdokimov IN, Fesan AA, Losev AP. New answers to the optical interrogation of asphaltenes: monomers and primary aggregates from steady state fluorescence studies. Energy Fuel 2016;30(6):4494–503. https://doi.org/10.1021/acs.energyfuels.6b00027.
[26] Behbahani JT, Miranbeigi AA, Sharifi K, Behbahani JZ. A New Investigation on asphaltene precipitation: experimental and a new thermodynamic approach. Pet Chem 2018;58(8):622–9. https://doi.org/10.1134/S0965544118080029.
[27] Wang J, Ferguson AL. Mesoscale simulation of asphaltene aggregation. J Phys Chem B 2016;120(32):8016–35. https://doi.org/10.1021/acs.jpcb.6b05925.
[28] Azari V, Abolghasemi E, Hosseini A, Ayatollahi S, Dehghani F. Electrokinetic properties of asphaltene colloidal particles: determining the electric charge using micro electrophoresis technique. Colloids Surf A Physicochem Eng Asp 2018;541:68–77. https://doi.org/10.1016/j.colsurfa.2018.01.029.
[29] Xia S, Veony E, Kostarelos K. A novel electro-deposition based asphaltene removal strategy. Fuel 2019;244(1–4):508–16. https://doi.org/10.1016/j.fuel.2019.01.175.
[30] Zhang L, Yang G, Wang JQ, Li Y, Li L, Yang C. Study on the polarity, solubility, and stacking characteristics of asphaltenes. Fuel 2014;128:366–72. https://doi.org/10.1016/j.fuel.2014.03.015.
[31] Rocha JWS, Vicente MA, Melo BN, Marques ML, Guimaraes RCL, Sad CMS, et al. Investigation of Electrical properties with medium and heavy brazilian crude oils by electrochemical impedance spectroscopy. Fuel 2019;241:42–52. https://doi.org/10.1016/j.fuel.2018.12.017.
[32] Charin RM, Chaves GMT, Kashefi K, Alves RP, Tavares FW, Nele M. Crude oil electrical conductivity measurements at high temperatures: Introduction of apparatus and methodology. Energy Fuel 2017;31(4):3669–74. https://doi.org/10.1021/acs.energyfuels.6b03237.
[33] Chen ZT, Zhang LH, Zhao SQ, Shi Q, Xu CM. Molecular structure and association behavior of petroleum asphaltene. Struct Bond 2016;168:1–38. https://doi.org/10.1007/430_2015.
[34] Poveda-Jaramillo JC, Molina-Velasco DR, Bohorques-Toledo NA, Torres MH, Ariza-León E. Chemical characterization of the asphaltenes from Colombian colorado light crude oil. Cien Technol Fut 2016;6(3):105–22. https://doi.org/10.29047/01225383.12.
[35] Banda EE, Padrón SI, Gallardo NV, Páramo U, Díaz NP, Melo JA. Physicochemical characterization of heavy oil and the precipitated asphaltenes fraction using UV spectroscopy and dynamic light scattering. J Eng Technol 2017;61(1):49–58.
[36] Riley BJ, Lennard C, Fuller S, Spikmans V. An FTIR method for the analysis of crude and heavy fuel oil asphaltenes to assist in oil fingerprinting. Forensic Sci Int 2016;266:555–64.
[37] Acevedo S, Gutierrez LB, Negrin G, Pereira JC, Delolme BMF, Dessalces G, et al. Molecular weight of petroleum asphaltenes: A comparison between mass spectrometry and vapor pressure osmometry. Energy Fuels 2005;19:1548–60. https://doi.org/10.1021/ef040071.
[38] Bouhadda Y, Bendedouch D, Sheu E, Krallafa A. Some Preliminary Results on a Physico-Chemical Characterization of a Hassi Messaoud Petroleum Asphaltene. Energy Fuel 2000;14(4):845–53. https://doi.org/10.1021/ef9902092.
[39] Mullins OC, Sabbah H, Eyssautier J, Pomerantz AE, Barre L, Andrews AB, et al. Advances in Asphaltene Science and the Yen–Mullins Model. Energy Fuel 2012;26:3986–4003. https://doi.org/10.1021/ef300185p.
[40] Martinez-Haya B, Hortal AR, Hurtado PM, Lobato MD, Pedrosa JM. Laser desorption/ionization determination of molecular weight distributions of polyaromatic carbonaceous compounds and their aggregates. J Mass Spectrom 2007;42:701–13. https://doi.org/10.1002/jms.1226.
[41] Ok S, Mal TK. NMR Spectroscopy analysis of asphaltenes. Energy Fuel 2019;33(11):10391–414. https://doi.org/10.1021/acs.energyfuels.9b02240.
[42] Rezaee NE, Heidarizadeh F, Sajjadifar S, Abbasi Z. Dispersing of Petroleum Asphaltenes by Acidic Ionic Liquid and Determination by UV-Visible Spectroscopy. Journal of Petroleum Engineering 2013;2013:1–5. https://doi.org/10.1155/2013/203036.
[43] Giraldo D, Chacón M, Ramirez JS, Blanco C, Combariza MY. Selective ionization by electron-transfer MALDI-MS of vanadyl porphyrins from crude oils. Fuel 2018;226:103–11. https://doi.org/10.1016/j.fuel.2018.04.016.
[44] Rodrigues CR, Hovell I, Lopez EM, Lopes AS, Rajagopal K. Characterization of functional groups of asphaltenes in vacuum residues using molecular modelling and FTIR techniques. Pet Sci Technol 2007;25(1–2):41–54. https://doi.org/10.1016/J.FUPROC.2005.10.010.
[45] Chacon Patino ML, Rowland SM, Rodgers RP. Advances in asphaltene petroleomics. part 1: Asphaltenes are composed of Abundant island and Archipelago structural motifs. Energy Fuel 2017;31(12):13509–18.
[46] Samedova FI, Mir-Babaev MF. High-molecular heteroatomic compounds of oils of Azerbaijan. Baku: Nefis; 1992. in Azerbaijan.
[47] Samadova FI. Oil of Azerbaijan. Baku: Elm; 2011. in Azerbaijan.
[48] Samedova FI, Guseinova BA, Aliev BM, Alieva FZ. Features of resins from oils of the Nizhnekura region of the South Caspian depression. Chem Technol Fuels Oils 2001;2:34–5. in Russia.
[49] Samedova F I, Rashidova S Yu, Aliev B M. Influence of the isolation method on the structural and group composition of naphthenic concentrates from Naftalan oil. Chemistry and technology of fuels and oils 2001; (5):29-34. (in Russia).
[50] Samedova FI, Zeynalova SA, Abdullaeva YA. Oils from new offshore fields. Chem Technol Fuels Oils 1998;4:34–6. in Russia.
[51] Samedova FI, Kasumova AM, Yu RS, Alieva VM. A New Method for Isolation of Asphaltenes from Petroleum and its Heavy Residues. Pet Chem 2007;47(6):432–5.
[52] Samedova FI, Mir-Babaev MF. Separation of asphaltenes by physical influence. Chem Technol Fuels Oils 1995;5:41–6. in Russia.
[53] Gonçalves MLA, Teixeira MAG, Pereira RCL, Mercury RLP, Matos JR. Contrıbutıon of thermal analysıs for characterızatıon of asphaltenes from Brazılıan crude oil. J Therm Anal Calorim 2001;64(2):697–706. https://doi.org/10.1023/A:1011588226768.
[54] Neuhaus N, Nascimento PTH, Moreira I, Scheer AP, Santos AF, Corazza ML. Thermodynamıc analysıs and modelıng of Brazılıan crude oıl and asphaltene systems: an experımental measurement and a pc-saft applıcatıon. Braz J Chem Eng 2019;36(1):557–71. https://doi.org/10.1590/0104-6632.20190361s20170575.
[55] Li G, Tan Y. The construction and application of asphalt molecular model based on the quantum chemistry calculation. Fuel 2022;308(4):1220–37. https://doi.org/10.1016/j.fuel.2021.122037.
[56] Ruiz-Morales Y. HOMO−LUMO gap as an index of molecular size and structure for polycyclic aromatic hydrocarbons (PAHs) and asphaltenes: A theoretical study. I. Chem A Eur J 2002;106(46):11283–308. https://doi.org/10.1021/jp021152e.
[57] Standard Test Method for Determination of Asphaltenes (Heptane Insolubles) in Crude Petroleum and Petroleum Products: ASTM International, ASTM D6560-12, 2018.
[58] Standard Test Method for Density, Relative Density, and API Gravity of Crude Oils by Digital Density Analyzer: ASTM International, ASTM D5002-22, 2022.
[59] Standard Test Method for Kinematic Viscosity of Transparent and Opaque Liquids (and Calculation of Dynamic Viscosity): ASTM International, ASTM D445-06, 2012.
[60] Standard Test Method for Sulfur in Petroleum and Petroleum Products by Energy Dispersive X-ray Fluorescence Spectrometry: ASTM International, ASTM D4294-21, 2021.
[61] Standard Test Method for Flash and Fire Points by Cleveland Open Cup Tester: ASTM International, ASTM D92-18, 2018.
[62] Standard Test Method for Freezing Point of Aviation Fuels: ASTM International, ASTM D2386-19, 2019.
[63] Yolchuyeva UJ, Japharova R, Vakhshouri AR, Khamiyev M, Salmanova Ch, Khamiyeva G. Photochemical investigation of aromatic hydrocarbons of Balakhani crude oil as petroleum luminophores. Appl Petrochem Res 2020;10(3):139–48. https://doi.org/10.1007/s13203-020-00253-9 1.
[64] Yolchuyeva UJ, Japharova R, Vakhshouri AR, Khamiyev M, Khamiyeva G. Investigation of photochemical conversion processes in aromatic hydrocarbons of Balakhani oil. J Pet Sci Eng 2021;196(1):1080–9. https://doi.org/10.1016/j.petrol.2020.108089.
[65] Yolchuyeva UJ, Japharova R, Khamiyev M, Alimardanova F. Investigation of Surakhani light crude oil compounds as a case study using modern spectroscopic techniques. J Pet Explor Prod Technol 2023. https://doi.org/10.1007/s13202-023-01702-6.
[66] Sergienko SR, Taimova BA, Talalaev EI. Vysokomolekulyarnye neuglevodorodnye soedineniya nefti [Nonhydrocarbon macromolecular compounds of oil]. Moscow: Nauka; 1979. in Russia.
[67] Asemani M, Rabbani AR. Oil-oil correlation by FTIR spectroscopy of asphaltene samples. J Geosciences 2016;20:273–83. https://doi.org/10.1007/s12303-015-0042-1.
[68] Ok S, Rajasekarana N, Sabtia MA, Josepha GA. Spectroscopic analysis of crude oil asphaltenes at molecular level. Pet Chem 2020;60(7):802–9. https://doi.org/10.1134/S0965544120070117.
[69] Brian KW, William TW, Graham RJ. Determination of Asphaltenes in Petroleum Crude Oils by Fourier Transform Infrared Spectroscopy. Energy Fuels 1998;12(5):1008–12. https://doi.org/10.1021/ef980078p.
[70] Al Humaidan FS, Hauser A, Rana MS, Lababidi HM. Impact of thermal treatment on asphaltene functional groups. Energy Fuel 2016;30(4):2892–903. https://doi.org/10.1021/acs.energyfuels.6b00261.

[71] Durand E, Clemancey M, Lancelin J, et al. Effect of chemical composition on asphaltenes aggregation. Energy Fuel 2010;24(2):1051–62. https://doi.org/10.1021/ef900599v.

[72] Parlov Vuković J, Novak P, Plavec J, Friedrich M, Marinić Pajc L, Hrenar T. NMR and chemometric characterization of vacuum residues and vacuum gas oils from crude oils of different origin. Croat Chem Acta 2015;88(1):89–95. https://doi.org/10.5562/cca2612.

[73] Parlov Vuković J, Novak P, Jednačak T. NMR Spectroscopy as a tool for studying asphaltene composition. Croat Chem Acta 2019;92(3):1851–60. https://doi.org/10.5562/cca3543.

[74] Rakhmatullin IZ, Efimov SV, Ya MB, Klochkov VV. Qualitative and quantitative analysis of oil samples extracted from some Bashkortostan and Tatarstan oilfields based on NMR spectroscopy data. J Pet Sci Eng 2017;156:12–8. https://doi.org/10.1016/j.petrol.2017.04.041.

[75] Sayil C, Ibis C. Synthesis and spectral properties of novel thionaphtoquinone dyes. Bull Kor Chem Soc 2010;31(5):1233–6. https://doi.org/10.5012/bkcs.2010.31.5.1233.

[76] Pathak P. Synthesis of S-alkyl/S-benzyl-1,4-dihydropyrimidines and evaluation of their biological activity. J Chem Pharm Res 2014;6(6):1207–11.

[77] Silva RC, Seidl PR. ^{1}H and ^{13}C NMR for Determining Average Molecular Parameters of Asphaltenes from Vacuum Residue Distillation. Ann Magn Reson 2004;3(3):63–7.

[78] Poveda JC, Molina DR, Pantoja-Agreda EF. ^{1}H- and ^{13}C-NMR structural characterization of asphaltenes from vacuum residua modified by thermal cracking. CT&F - Ciencia, Tecnología y Futuro 2014;5(4):49–60. https://doi.org/10.29047/01225383.40.

[79] Morgan TJ, Alvarez-Rodriguez P, George A, Herod AA, Kandiyoti R. Characterization of Maya Crude Oil Maltenes and Asphaltenes in Terms of Structural Parameters Calculated from Nuclear Magnetic Resonance (NMR) Spectroscopy and Laser Desorption-Mass Spectroscopy (LD-MS). Energy Fuel 2010;24(7):3977–89. https://doi.org/10.1021/ef100320t.

[80] Ok S, Mahmoodinia M, Rajasekaran N, Sabti MA, Lervik A, Cabriolu R. Molecular structure and solubility determination of asphaltenes. Energy Fuel 2019;3(9):8259–70. https://doi.org/10.1021/acs.energyfuels.9b01737.

[81] Pyase LG, Prem VD, Rakesh KK, Pradeep K. Estimation of average structural parameters of petroleum crudes and coal-derived liquids by ^{13}C and ^{1}H NMR. Fuel 1986;65:515–9.

[82] Juan CP, Daniel RM. Average molecular parameters of heavy crude oils and their fractions using NMR spectroscopy. J Pet Sci Eng 2012;84–85:1–7. https://doi.org/10.1016/j.petrol.2012.01.005.

[83] Qian SA, Li CF, Zhang PZ. Study of structural parameters on some petroleum aromatic fractions by ^{1}H NMR/IR and ^{13}C, ^{1}H NMR spectroscopy. Fuel 1984;63(2):268–73. https://doi.org/10.1016/0016-2361(84)90049-8.

[84] Kök MV, Varfolomeev MA, Nurgaliev DK. Determination of SARA fractions of crude oils by NMR technique. J Pet Sci Eng 2019;179:1–6. https://doi.org/10.1016/j.petrol.2019.04.026.

[85] Zheng C, Zhu M, Zhang D. Characterisation of Asphaltenes Extracted from an Indonesian Oil Sand Using NMR. DEPT and MALDI-TOF Energy Procedia 2015;75:847–52.

[86] Díaz-Sánchez H, Rojas-Trigos BJ, Leyva C, Trejo-Zárraga F. An approach for determination of asphaltene crystallite by X-ray diffraction analysis: A case of study. Petroleum science and technology 2017;35(13):1415–20. https://doi.org/10.1080/10916466.2017.1336771.

[87] Humaidan FS, Hauser A, Rana MS. Changes in asphaltene structure during thermal cracking of residual oils: XRD study. Fuel 2015;150:558–64. https://doi.org/10.1016/j.fuel.2015.02.076.

[88] Odebunmi EO, Adeniyi SA. Infrared and ultraviolet spectrophotometric analysis of chromatographic fractions of crude oils and petroleum products. Journal Bulletin of the chemical society of Ethiopia 2007;21(1):135–40. https://doi.org/10.4314/BCSE.V21I1.61394.

[89] El-Bassoussi AA, El Sayed SM, El Anmed MH, Basta JS, Attia ESK. Characterization of some local petroleum residues by spectroscopic techniques. Pet Sci Technol 2010;28(5):430–44. https://doi.org/10.1080/10916460902744554.

[90] Banda-Cruz EE, Gallardo-Rivas NV, Martínez-Orozco RD, Páramo-García U, Mendoza-Martínez AM. Derivative UV-VIS spectroscopy of crude oil and asphaltene solutions for composition determination. J Appl Spectrosc 2021;87(6):1157–62. https://doi.org/10.1007/s10812-021-01124-4.

[91] Gouterman M. Spectra of porphyrins. J Mol. Spectroscopy 1961;6:138–63. https://doi.org/10.1016/0022-2852(61)90236-3.

[92] Giovannetti R. The Use of Spectrophotometry UV-Vis for the Study of Porphyrins. In: Uddin J, editor. Macro To Nano Spectroscopy. Publisher: InTech; 2012. p. 87–107.

[93] Davarpanah L, Vahabzadeb F, Dermanaki A. Structural study of asphaltenes from Iranian heavy crude oil. Oil Gas Sci Technol 2015;70(6):1035–49. https://doi.org/10.2516/ogst/2012066.

[94] Kejing Li, Monica Vasiliu, Casey R. McAlpin, Yuan Yang, David A Dixon, Kent J Voorhees, Michael Batzle, Matthew W Liberatore, Andrew M Herring. Further insights into the structure and chemistry of the Gilsonite asphaltene from a combined theoretical and experimental approach. Fuel 2015; 157:16–20. DOI: 10.1016/j.fuel.2015.04.029.

[95] Banda EE, Rivas NV, Páramo U, Estrada IA, Pozas D, Reyes J. Crude oil aggregation by microscopy and dynamic light scattering. Pet Sci Technol 2016;34(22):1812–917. https://doi.org/10.1080/10916466.2016.1230754.

[96] Agrawala M, Yarranton HW. An asphaltene association model analogous to linear polymerization. Ind Eng Chem Res 2001;40(21):4664–72. https://doi.org/10.1021/ie0103963.

[97] Sh WS, Yang Chuang XCM, Zhao SQ, Quan S. Separation and characterization of petroleum asphaltene fractions by ESI FT-ICR MS and UV-vis spectrometer. Sci China Chem 2013;56(7):856–62. https://doi.org/10.1007/s11426-013-4900-2.

[98] Yu DM, Mukayeva GR. The method of determining the ionization potentials and the electron affinity of atoms and molecules by electron spectroscopy. J Appl Spectrosc 1992;56(4):570–4.

[99] Yu DM, Shulyakovskaya DO, Mukaeva GR, Yarmukhametova GU, Latypov KF. Simple characteristics estimation methods of material and molecule electronic structure. J Mater Sci Eng 2012;2(4):261–8.

[100] Nalwaya V, Piumsomboon P, Fogier S. Studies on asphaltenes through analysis of polar fractions. Ind Eng Chem Res 1999;38(3):964–72. https://doi.org/10.1021/ie9804428.

[101] Korneev DS, Pevneva GS. Thermal Transformations of Asphaltenes at a Temperature of 120°C. Journal of Siberian Federal University Chemistry 2019;12(1):101–17. https://doi.org/10.17516/1998-2836-0110.

[102] Boytsova A, Kondrasheva N, Ancheyta J. Thermogravimetric determination and pyrolysis thermodynamic parameters of heavy oils and asphaltenes. Energy Fuels 2017;31(10):10566–75. https://doi.org/10.1021/acs.energyfuels.7b01584.

[103] Paridar S, Nazar ARS, Karimi Y. Experimental evaluation of asphaltene dispersants performance using dynamic light scattering. J Pet Sci Eng 2018;163:570–5. https://doi.org/10.1016/j.petrol.2018.01.013.

[104] Solaimany-Nazar AR, Rahimi H. Dynamic Determination of Asphaltene Aggregate Size Distribution in Shear Induced Organic Solvents. Energy Fuel 2008;22(5):3435–42. https://doi.org/10.1021/ef800173s.

[105] Peng B, Yuan L, Tang X, Wang Y, Li Y, Liua W, et al. Molecular dynamics simulations of aggregation and viscosity properties of model asphaltene molecules containing a polycyclic hydrocarbon nucleus with toluene additive under shear interactions. RSC Adv 2024;14(4):2577–89. https://doi.org/10.1039/D3RA06483B.

[106] Khalaf MH, Mansoori GA. A new insight into asphaltenes aggregation onset at molecular level in crude oil (an MD simulation study). J Pet Sci Eng 2018;162:244–50. https://doi.org/10.1016/j.petrol.2017.12.045.

[107] Neese F. The ORCA program system. Wiley Interdiscip Rev: Comput Mol Sci 2011;2(1):73–8. https://doi.org/10.1002/wcms.1327.

[108] Choudhary V, Bhatt A, Dash D, Sharma N. DFT calculations on molecular structures, HOMO-LUMO study, reactivity descriptors and spectral analyses of newly synthesized diorganotin (IV) 2-chloridophenylacetohydroxamate complexes. J Comput Chem 2019;40(27):2354–63. https://doi.org/10.1002/jcc.26012.

[109] Ayalew M. DFT Studies on Molecular Structure, Thermodynamics Parameters, HOMO-LUMO and Spectral Analysis of Pharmaceuticals Compound Quinoline (Benzo[b]Pyridine). J Biophys Chem 2022;13(3):29–42. https://doi.org/10.4236/jbpc.2022.133003.

[110] Verma C, Quraishi MA. Ionic liquids-metal surface interactions: Effect of alkyl chain length on coordination capabilities and orientations. e-Prime - Advances in Electrical Engineering. Electronics and Energy 2022;2(100070). https://doi.org/10.1016/j.prime.2022.100070.

[111] Miar M, Shiroudi A, Pourshamsian K, Oliaey AR, Hatamjafari F. Theoretical investigations on the HOMO–LUMO gap and global reactivity descriptor studies, natural bond orbital, and nucleus-independent chemical shifts analyses of 3-phenylbenzo[d]thiazole-2(3H)-imine and its para-substituted derivatives: Solvent and substituent effects. J Chem Res 2021;45(1–2):147–58. https://doi.org/10.1177/1747519820932091.

[112] El-Shamy NT, Alkaoud AM, Hussein RK, Ibrahim MA, Alhamzani AG. Mortaga M Abou-Krisha. DFT, ADMET and Molecular Docking Investigationsfor the Antimicrobial Activityof 6,60-Diamino-1,10,3,30-tetramethyl-5,50-(4-chlorobenzylidene)bis[pyrimidine-2,4(1H,3H)-dione]. Molecules 2022;27(3):620. https://doi.org/10.3390/molecules27030620.